High- and low-affinity sulfate reduction kinetics expressed in a marine sulfate-reducing bacterium, *Desulfobacterium autotrophicum*

Running title: High-affinity sulfate reduction in *D. autotrophicum*

Irene Harder Tarpgaard, Bo Barker Jørgensen, Kasper Urup Kjeldsen and Hans Røy[1]

Center for Geomicrobiology, Department of Bioscience,

Aarhus University, Ny Munkegade 114-116, 8000 Aarhus C, Denmark

[1]Corresponding author: hans.roy@bios.au.dk; phone: +45-87155985

Keywords: *Desulfobacterium autotrophicum* HRM2; DSMZ 3382; sulfate reduction; affinity; kinetics; sulfate uptake, membrane transport; sulfate-reducing bacteria, gene expression.

ABSTRACT

Previous studies of the kinetics of dissimilatory sulfate reduction in marine sediment have shown that marine sulfate-reducing bacteria (SRB) can reduce sulfate with both high and low sulfate half-saturation constants. So far, however, all marine pure cultures that have been investigated have shown only low-sulfate affinity sulfate reduction kinetics. It remains unknown whether the high sulfate-affinity marine sulfate reduction is catalyzed by unknown SRB or whether known SRB possess unrecognized high-affinity sulfate reduction systems. We used ^{35}S-sulfate incubation experiments to show that cultures of *Desulfobacterium autotrophicum* will switch from low-affinity to high-affinity sulfate reduction when sulfate concentrations fall below 500 μM. The mean apparent half saturation constant (K_m) was 150 μM at high sulfate concentrations and 8 μM at low sulfate concentration. The high-affinity K_m value is comparable to K_m values found in SRB inhabiting freshwater sediments. *D. autotrophicum* cultures could deplete sulfate to less than 25 nM and we could not detect a lower concentration threshold for reduction of sulfate. The switch in K_m value was accompanied by a change in the expression level of genes encoding membrane-bound transport proteins putatively involved in sulfate uptake in *D. autotrophicum* whereas the genes encoding dissimilatory adenosine-5'-phosphosulfate reductase and sulfite reductase, the two key enzymes of the dissimilatory sulfate reduction pathway, were constitutively expressed at both high and low sulfate concentrations. Our results demonstrate that a marine sulfate reducer can efficiently reduce sulfate at both high and low sulfate concentrations, possibly by activation of different sulfate transporters in the membrane.

INTRODUCTION

Sulfate-reducing bacteria (SRB) constitute a microbial guild of key environmental significance, as dissimilatory sulfate reduction is the main driver of terminal organic matter mineralization in the anoxic seabed (1). Sulfate reduction occurs in the sulfate-rich surface sediment (2), in the sulfate-depleted sulfate-methane transition zone (SMTZ) (3), and even below this zone as part of a cryptic sulfur cycle (4). SRB depend on sulfate as their electron acceptor and therefore possess a fast and energy-efficient sulfate uptake mechanism (5). The uptake systems seemingly operate across a wide range of sulfate concentrations, thus enabling the persistence of SRB above, within and below the SMTZ in marine sediments. The rate of sulfate reduction at a given sulfate concentration depends on the properties of both the membrane-bound sulfate transporter(s) and the enzymes involved in sulfate activation and reduction although the kinetics of these individual steps are unresolved. The apparent half-saturation constant (K_m) relates the rate of sulfate reduction in living microbes to the external substrate concentration (6). Sulfate reduction that operate with a low K_m is eficient at low sulfate concentrations, and is defined as having high affinity kinetics. Vice versa, sulfate reduction that operate with a higher K_m is more sensitive to low sulfate concentrations and is defined as having relatively low affinity kinetics. We have demonstrated that two distinct K_m values of 400 μM at high sulfate concentrations, and down to 2-4 μM upon sulfate limitation/depletion exist in sulfate-rich marine surface sediments (7). High-affinity sulfate reduction is known from pure cultures of freshwater SRB, which have K_m <10 μM (8-12). The only marine SRB, for which apparent sulfate affinities are reported, *Desulfovibrio salexigens* and *Desulfobacter postgatei*, exhibit high K_m values of 77 μM and 200 μM, respectively, and thus seem only to possess low-affinity sulfate reduction kinetics (10, 13).

59 Indirect evidence for high-affinity sulfate reduction kinetics in pure cultures of marine SRB was
60 established from measurements of sulfate accumulation upon inhibition of sulfate reduction. Both
61 freshwater and marine species of SRB were shown to accumulate sulfate when incubated in sulfate-
62 depleted medium whereas little accumulation occurred at high sulfate concentrations suggesting the
63 coexistence of two different sulfate uptake systems (5, 14-16). As a general mechanism for sulfate
64 uptake it was proposed that the accumulation at low external sulfate concentrations was driven by a
65 symport mechanism where three H^+ or Na^+ ions were cotransported per SO_4^{2-} and the low
66 accumulation at high external sulfate concentrations was driven by symport where only two H^+ or
67 Na^+ ions were cotransported. The kinetics of uptake and reduction, i.e. the apparent half saturation
68 constants (K_m) of the processes, were not investigated. The shift in sulfate accumulation in several
69 pure cultures at the same concentration treshold (5, 14-16) and the shift in K_m in marine mud (7),
70 however, suggests a connection.

71 Neither the proteins that transport sulfate across the cell membrane of SRB, nor the genes coding
72 for them, are known. We must, therefore, infer information about these transporters from the sulfate
73 uptake systems involved in the assimilatory sulfate reduction which have been characterized. In
74 bacteria, known sulfate transporters driven by an electrochemical potential across the cytoplasmic
75 membrane can be classified into three transporter families (17): (i) The Sulfate Permease (SulP)
76 Family (TC 2.A.53). (ii) The Divalent Anion:Na^+ Symporter (DASS) Family (TC 2.A.47). (iii) The
77 Inorganic Phosphate Transporter (CysP/PiT) Family (TC 2.A.20). Based on genome sequence data
78 SRB harbor several SulP and DASS family homologs and typically only the SulP-encoding genes
79 are assigned a role in sulfate uptake in the genome annotations.

80 We used the marine sulfate reducer, *Desulfobacterium autotrophicum* HRM2 (DSMZ 3382) (18)
81 as a model organism to resolve whether marine SRB have the capacity for high-affinity

dissimilatory sulfate reduction and to investigate how *D. autotrophicum* adjust its apparent sulfate reduction kinetics to the external sulfate concentration. Initial results indeed identified dual kinetics in *D. autotrophicum* with a shift in apparent K_m at a sulfate concentration around 500 μM. We therefore continued to profile the expression of eight putative sulfate transporter-encoding genes encoded in its genome (19) to identify the transporter(s) involved in sulfate uptake and thus illuminate mechanism behind the kinetic flexibility.

MATERIALS AND METHODS

Batch cultures grown at high sulfate concentrations

D. autotrophicum HRM2^T (DSMZ 3382^T, T=type strain) was grown in batch culture at 28 °C in a marine medium (DSMZ 383) with ethanol or lactate (10-20 mM) as electron donor and sulfate (20 mM) as electron acceptor. For kinetic experiments, cultures (100 mL) in exponential growth phase were harvested by centrifugation (11,000 RCF) for 20 min at 4 °C under a sterile N_2:CO_2 (9:1, v/v) atmosphere. The supernatant was decanted under a flow of sterile N_2:CO_2 gas (9:1, v/v) and fresh anoxic medium (DSMZ 383, devoid of sulfate and electron donor, pH 7.1) was added for a second centrifugation (10,000 RCF) for 10 min at 4 °C. After the second washing step the supernatant was again decanted and cells were resuspended in 60 mL of the anoxic substrate-free medium under a sterile N_2:CO_2 gas (9:1, v/v) atmosphere in 120 mL serum bottles. The bottles were then capped with butyl rubber stoppers and crimp sealed, ethanol was added to a final concentration of 1 mM, and the pH was adjusted to 7.1. The washed cells were pre-incubated at 28 °C until all residual sulfate was used (<24h), as verified by ion chromatographic measurements (see below), before being used for experiments.

105 **Fed batch cultures grown at low sulfate concentrations**

106 *D. autotrophicum* was grown at constant and low sulfate concentration with a fed batch system at
107 28°C. For each fed batch culture, 100 mL cell culture was washed by centrifugation as described
108 above. Afterwards the cell pellet was resuspended in 400 mL DSMZ 383 medium without sulfate or
109 electron donor in 500 mL Pyrex bottles closed with a rubber stopper under a sterile N_2:CO_2 gas
110 (9:1, v/v) atmosphere. Next, 1 mM ethanol was added and the sulfate concentration was monitored
111 by ion chromatography to ensure that all residual sulfate was being consumed. After depletion of
112 the residual sulfate, substrates were added to the culture by a double syringe pump. Two 50 mL gas
113 tight BD plastic syringes with the anoxic DSMZ 383 medium, one containing sulfate and one
114 containing ethanol (3:2 molar ratio), were connected to the culture bottle by polyether ether ketone
115 (PEEK) tubing (inner diameter 0.5 mm). The two substrates were then added at a constant rate such
116 that the addition of sulfate was slightly slower than the rate of sulfate depletion measured during the
117 pre-incubation (28 ^{o}C). Thus, the sulfate was consumed at near the same rate as before but the
118 concentration was cept constantly near zero by the cells. The sulfate concentration was monitored
119 during the experiment along with pH to assure that the cultures were growing under constant sulfate
120 limitation (28 ^{o}C). Cell densities were determined at the beginning and the end of the cultivation by
121 counting of SYBR Gold stained cells under a fluorescence microscope (20). The cultures were
122 subsequently used directly in initial-velocity experiments and in progress curve experiments with no
123 washing.

124

125 **Progress curve experiments at low sulfate concentrations**

126 Sulfate reduction rates below 100 μM sulfate concentrations were investigated during progressive
127 depletion of sulfate. Such progress curve experiments were initiated by adding 70-100 μM final

concentration of sulfate and 1 MBq $^{35}SO_4^{2-}$ sulfate tracer to sulfate-depleted batch or fed batch cultures (28 °C). Subsamples of 900 µL were subsequently withdrawn at 15-30 min intervals with 1 mL N_2-flushed syringes. 500 µL was transferred into 1.5 mL plastic tubes containing 500 µL 5% zinc acetate (wt/vol) solution to precipitate H_2S as ZnS. The samples were briefly vortex mixed and centrifuged (13,400 rpm for 7 min) to separate out ZnS, and 800 µL supernatant was transferred to a new 1.5 mL plastic tube for a second centrifugation step (13,400 rpm for 5 min). Finally 500 µL supernatant was transferred to vials containing 10 mL scintillation fluid (Ecoscint) to measure the radioactivity of the residual dissolved sulfate in counts per minute (cpm). The use of two centrifugation steps was nessesary for complete separation of the dissolved $^{35}SO_4^{2-}$ from the reduced ^{35}S-pools contained in the solid phase (see below). The remaining 400 µL culture in the syringes was filtered through 0.22 µm pore size filters; sulfide was removed from the filtrates by bubbling with humidified CO_2 and filtrates were stored at 4°C for subsequent ion chromatographic sulfate analysis (see below). The primary results from progress curve experiments were curves of sulfate concentration as function of time during sulfate depletion.

Initial-velocity experiments at high sulfate concentrations

Sulfate reduction rates at medium and high sulfate concentrations from 80 µM to 20 mM were determined in short incubations (28 ^{o}C) at quasi-constant sulfate concentrations, referred to as initial-velocity experiments. Cells for initial-velocity experiments were grown in fed batch as described above. Ethanol (1 mM) was added to 100 mL stock culture before 1 mL or 3 mL subsamples were transferred to Hungate tubes containing 5 mL or 3 mL anoxic sulfate-free medium DSM 383 for experiment I and II, respectively. Hungate tubes were left for one hour at 28 °C below a sterile N_2:CO_2 (9:1, v/v) atmosphere before sulfate was added to final concentrations ranging from 0.08 to 20 mM to cover a wide range of initial sulfate concentrations.

Subsamples of 400 µL were withdrawn for sulfate concentration measurements (as described above) from the tubes just before $^{35}SO_4^{2-}$ tracer was added to provide positive control of the initial sulfate concentration. Then $^{35}SO_4^{2-}$ tracer (100 kBq) was injected into each Hungate tube. The cultures were incubated for two hours at 28°C. Sulfate reduction was stopped at the end of the incubation by mixing the cultures with two mL zinc acetate (20 % wt/vol) and immediate freezing at -20°C. The frozen cultures were later treated by cold chromium-reduction distillation to separate sulfate from the reduced products of sulfate reduction (21). Sulfate reduction rates (SRR) were calculated according to:

$$SRR = [sulfate] \times (^{35}S\text{-TRIS} / ^{35}S\text{-sulfate}) \times (1.06/t)$$

where [sulfate] is the sulfate concentration in the culture at the beginning of the experiments (µM), ^{35}S-TRIS is the radioactivity of total reduced inorganic sulfur (TRIS) at the end of incubation in counts per minute (cpm), ^{35}S-sulfate is the radioactivity of sulfate added to the culture (cpm), 1.06 is a correction factor for the expected isotope discrimination against ^{35}S-sulfate versus the bulk ^{32}S-sulfate by SRB, and t is the incubation time measured in hours (22). The primary result of initial velocity experiments was curves of sulfate reduction rate as function of sulfate concentration.

Kinetic parameters

The kinetic parameters, V_{max} and K_m were estimated by non-linear parametric fits directly to measured rates versus concentration plots (initial-velocity experiments) or concentrations versus time plots (progress curves) as described by Tarpgaard et al, 2011 (7) using the Michaelis-Menten (MM) rate equation

$$V(C) = V_{\max} \frac{C}{K_m + C} \quad \text{(Equation 1)}$$

where C is the sulfate concentration, $V(C)$ is the sulfate reduction rate as function of sulfate concentration, V_{max} is the maximum sulfate reduction rate at high substrate concentration, and K_m is the apparent half saturation constant.

The rates from the initial-velocity experiments were compared directly to the MM rate equation (Eq 1) where V_{max} and K_m were varied until the best fit was achieved (smallest sum of squared deviations between measured and calculated rates). The kinetic parameters in the progress curve experiments were found by fitting data to the differential equation that describes the progressive depletion of sulfate over time when the rate is controlled by Eq 1:

$$C(t) = C_0 - \int V_{\max} \frac{C}{(K_m + C)} dt \quad \text{(Equation 2)}$$

where, $C(t)$ is the concentration as function of time and C_0 is the start concentration.

Sulfate measurements

Sulfate concentrations down to 1 µM were determined by ion chromatography (IC) on a Dionex ICS 2500 equipped with an AS 18 column with KOH as eluent (step profile from 12 to 30 mM) (21), and on a Dionex IC-3000 2-dimensional IC equipped with the columns AS24 & AS11 with 19 mM KOH as eluent.

To determine micromolar to sub-micromolar concentrations of sulfate, standards were prepared with the same concentration of NaCl as in the samples to be analyzed. The supernatant samples

192 drawn from the progress curve experiments were diluted 2-fold. For the initial-velocity
193 experiments, samples were diluted in Milli-Q water to ≤400 μM sulfate.

194 The ratio of sulfate radioactivity to sulfate concentration was established at the start of each
195 progress curve experiment. The sulfate concentration during depletion could then be calculated with
196 high precision and sensitivity from the residual sulfate radioactivity and could, in addition, be
197 calibrated against the IC-derived concentration data to obtain high accuracy.

198

199 **Gibbs free energy**

200 Sulfate reduction coupled to complete ethanol oxidation follows the stoichiometric equation:

201 $2C_2H_5OH + 3SO_4^{2-} \rightarrow 4HCO_3^- + 3HS^- + H^+ + 2H_2O$ (Equation 3)

202 The change in Gibbs free energy, ΔG_r during the reaction was calculated at pH 7.1 and 28 °C
203 according to:

204 $$\Delta G_r = \Delta G^o + RT \ln\left(\frac{[HCO_3^-]^4[HS^-]^3[H^+][H_2O]^2}{[C_2H_5OH]^2[SO_4^{2-}]^3}\right)$$ (Equation 4)

205 where $\Delta G°$ is calculated under standard conditions, R is the gas constant (0.008314 kJ mol^{-1} K^{-1}),
206 and T is the absolute temperature during the experiments. The small difference in $\Delta G°$ between the
207 25 °C of standard conditions and the 28 °C of the experiment was ignored.

208

209 **RNA extraction**

Cultures (50 mL) growing at high sulfate concentrations (15 mM) with excess ethanol or lactate were harvested by centrifugation (11,000 RCF) for 4 min at 4 °C under an sterile N_2:CO_2 (9:1, v/v) atmosphere in Falcon tubes. The supernatant was quickly decanted and the pellets snap-frozen in liquid N_2 and stored at -80 °C until RNA extraction. Cells subjected to low sulfate concentrations (<70 μM) were initially centrifuged and resuspended in 50 mL of sulfate-free medium under an N_2:CO_2 (9:1, v/v) atmosphere. Ethanol or lactate was added (1 mM) and after one to three days all residual sulfate was depleted as inferred from IC measurements. Additional sulfate (10-70 μM) was added and the cells were allowed to respire sulfate for a few hours before they were harvested for RNA extraction as described for the high sulfate concentration cultures above. Cultures used for progress curves were harvested for RNA extraction immediately after complete sulfate depletion at the end of the experiments.

Cell pellets used for RNA extraction were thawed on ice upon addition of 100-500 μL RNAprotect Bacteria reagent (Qiagen). Total RNA was extracted using the RNeasy Mini Kit (Qiagen). Cells were lyzed by lysozyme treatment according to the RNeasy Mini Kit protocol followed by mechanical disruption in a lysing Matrix E tube from the Fast DNA Spin kit for soil (MP biomedicals) with a Tissuelyser (Qiagen) at 50 oscillations sec^{-1} for 20 sec. Residual DNA was removed from purified RNA by DNase treatment for 30 min at 37 ^{o}C (Turbo DNase, Ambion) followed by a final RNA clean up step with the RNeasy Mini Kit (Qiagen). The amounts of RNA extracted were quantified with the Qubit RNA BR Assay Kit (LifeTechnologies).

Gene identification, primer design and RT-PCR

With the IMG online platform (23) the *D. autotrophicum* HRM2 genome was searched for encoded proteins matching PFAM and TIGRFAM models (24, 25) of protein families with members that

represent known membrane-bound sulfate transport proteins (17): (i) The SulP Family (TC 2.A.53) targeted by TIGR00815 and PFAM00916. (ii) The DASS Family (TC 2.A.47) targeted by TIGR00785, PFAM00939. (iii) The CysP/PiT Family (TC: 2.A.20) targeted by PFAM01384. (iv) The ATP-dependent sulfate/thiosulfate ABC transporter CysPTWA (TC 3.A.1.6.1) targeted by TIGR00968, TIGR00969 and TIGR00971. Because no specific PFAM models exist for CysPTWA the genome was also searched for CysPTWA homologs with the COG (models COG1118, COG4208, COG1613 and COG4150) for this transporter (26). The *D. autotrophicum* genome was furthermore searched for homologs of the putative membrane-bound sulfate transporter CysZ known from *E. coli* and *Corynebacterium glutamicum* (27, 28) by Blastp searches (29) with the CysZ protein sequences of *E. coli* and *C. glutamicum* as queries. However, no positive hits were obtaining with an e-value cutoff of 10^{-5}.

Three SulP family transporters (HRM2_33490, HRM2_13280, HRM2_40360) and five DASS family transporters (HRM2_07790, HRM2_38230, HRM2_38270, HRM2_38300, HRM2_40290) were identified in the *D. autotrophicum* genome. Known sulfate transporters of the DASS family are mostly eukaryotic while characterized bacterial members transport dicarboxylic acids. However, recently a DASS family permease of *Rhodobacter capsulatus* was shown to transport sulfate demonstrating that bacterial members of this family may also mediate sulfate uptake (30). The CysP/PiT family members are known to transport phosphate, but include also one sulfate transporter, CysP of *Bacillus subtilis* (31). As *D. autotrophicum* possesses only one gene which belongs to this family (HRM2_22920) and which shares little similarity with, and is twice the length of, the *B. subtilis* CysP we assume that HRM2_22920 is involved in phosphate rather than sulfate uptake. The *D. autotrophicum* genome does not encode proteins representing the ATP-dependent sulfate uptake system which is accordance with the previous observation that accumulation of sulfate in *D. autotrophicum* was not correlated with the cellular ATP content (14).

257 Eight primer sets were designed for the SulP and DASS family sulfate transporter-encoding
258 genes identified in the *D. autotrophicum* genome along with three other primer sets respectively
259 targeting the genes *dsrB*, *aprA* and *rpoB* (Table 1). The specificity and annealing temperatures of
260 the primers were tested on DNA extracted from a *D. autotrophicum* culture with the PowerLyzer
261 PowerSoil DNA Isolation Kit (MOBIO) according to the manufactures protocol. Temperature
262 gradient PCR was carried out in 25 µL reaction mixtures containing 0.5 µL DNA template, 0.5µL
263 of each primer, (10 pmol μl^{-1}) 12.5 µL Taq Polymerase Master Mix Red (Ampliqon) and 11 µL
264 dH_2O. Thermal cycling consisted of 5 min initial denaturation at 93 °C followed by 27 cycles of 92
265 °C for 45 s, 48-58 °C for 45 s, 72 °C for 60 s and a final extension at 72 °C for 10 min. PCR
266 products were evaluated on 1.5 % (wt/vol) agarose gels. All primers produced a single amplification
267 product of the expected size. The temperature gradient PCR showed 57 ^{o}C to represent an
268 appropriate annealing temperature for all primer pairs.

269 Reverse transcription (RT)-PCR was carried out in 25 µL reaction mixtures with 2.5 µL DNAse
270 treated RNA template containing 2.5 ng μL^{-1} RNA and 0.5 µL of each primer (10 pmol μl^{-1}) by the
271 One Step RT-PCR Kit (Qiagen). Thermal cycling consisted of a 30 min initial RT step at 50 °C
272 followed by 15 min incubation at 95 °C prior to initiation of 27 PCR cycles of 94 °C for 45 s, 57 °C
273 for 45 s, 72 °C for 45 s, and a final extension at 72 °C for 10 min. The absence of contaminating
274 DNA in the RNA extracts was confirmed by parallel PCR reactions with primer pairs respectively
275 targeting the *dsrB*, *aprA*, *rpoB* and 16S rRNA genes (Table 1). These PCR reactions were
276 performed with the Hot StarStarTaq Master Mix Kit (Qiagen), which is based on the same Taq
277 polymerase as the OneStep RT-PCR Kit. Reaction conditions and thermal cycling were the same as
278 used for the RT-PCR except that the initial 30 min RT step was omitted. RT-PCR products were
279 evaluated by 1.5 % (wt/vol) agarose gel electrophoresis and band intensities were used as proxy for
280 gene expression level upon staining of gels with SYBRGold.

RESULT

Progress curves

Sulfate consumption of *D. autotrophicum* followed simple MM type saturation kinetics when subjected to sulfate concentrations below 100 μM. A typical progress curve for *D. autotrophicum* is presented in Fig. 1. Depending on the cell densities the maximum sulfate reduction rate in these experiments varied from 12 to 43 μM h^{-1}. The depletion of sulfate was near linear over time down to 10-15 μM sulfate. The mean half saturation concentration, K_m, was 8 μM (±2.6 S.D.) in 7 progress curve experiments, as determined by fitting the data from progressive depletion of sulfate to Eq 1. The concentration of sulfate supplied during growth of the culture (15 mM in batch or 2-400 μM in fed batch) did not influence K_m or cell-specific V_{max}. The type of electron donor supplied during growth of the cultures (ethanol or lactate) did not influence K_m for sulfate either. However, all kinetic experiments were conducted with ethanol as only electron donor to avoid the potential for bias caused by partial oxidation of lactate during these.

At sulfate concentrations below 1-2 μM the rate of depletion of ^{35}S leveled further off and after 6-12 h of incubation a small but constant pool of radioactivity remained in supernatants upon separation of sulfate and zinc-precipitated sulfide by centrifugation. This pool was equivalent to 0.1-2 μM sulfate based on the initial sulfate concentrations. To determine if the ^{35}S-radioactivity that remained in the supernatants was indeed residual ^{35}S-sulfate or if it could be ^{35}S-sulfide that had not been removed by precipitation, the supernatants from nine experiments were subjected to cold chromium-reduction distillation. For these distillations the residual ^{35}S-sulfide pool was determined by scintillation counting on reduced distillate trapped as zinc sulfide, while the ^{35}S-sulfate pool was determined in the remaining chrome-acid reagents after distillation. The calculated

304 mean residual sulfate was 26 nM (±23 nM), i.e. insignificant for the kinetic experiment. The
305 constant pool of radioactivity that remained after 6-12 h was therefore not ^{35}S-sulfate but rather
306 residual ^{35}S-sulfide not removed by precipitation and centrifugation.

307 The decrease in sulfate radioactivity over time was equivalent to the net sulfate reduction to
308 sulfide, as the decrease in ^{35}S sulfate was mirrored by an increase in ^{35}S TRIS (Fig. 2). The mean
309 total ^{35}S tracer recovery was only 96 % due to incomplete separation of ^{35}S TRIS in the first
310 centrifugation from which samples were taken for this analysis. We analyzed both the sulfate
311 radioactivity and the sulfate concentration to test whether the decrease in sulfate radioactivity over
312 time was proportional to the decrease in the free sulfate pool. The latter, measured by ion
313 chromatography, showed a similar decrease as the former, thus confirming that the sulfate
314 radioactivity was proportional to the sulfate concentration throughout the experiment. The depletion
315 of sulfate could be followed by ion chromatography down to 2.5 μM when sulfide was removed
316 with CO_2 immediately after sampling. As a methodological observation, sulfate formed from
317 oxidation of sulfide could be up to 30 μM when samples were not flushed immediately with CO_2.

318

319 **Initial-velocity experiments combined with progress curves**

320 Sulfate reduction rates in the initial-velocity experiments resembled MM kinetics at concentrations
321 above 1mM sulfate, but with a lower apparent K_m than what was observed in progress curve
322 experiments. Fig. 3a shows a combined plot of initial-velocity experiment data from fed batch
323 cultures I and II and progress curve data generated from fed batch experiment II (also shown in Fig.
324 1) with rates expressed as cell-specific sulfate reduction rates at all concentrations tested. The
325 combination of progress curve and initial-velocity experiments made it possible to measure the
326 sulfate reduction rate across a broad range of sulfate concentrations. Note that cell-specific sulfate

reduction rates from the two methods agree in the concentration range that was covered by both methods. Fig. 3a shows the entire sulfate concentration range, 1-20 mM, of the experiments but it is very difficult to distinguish sulfate reduction rates at sulfate concentrations below 1 mM. Fig. 3b shows rates in the range from 0-1 mM sulfate and identify the high-affinity sulfate reduction at the low concentration range that was revealed by the progress-curve experiments already. When the cell-specific sulfate reduction rates is plotted against sulfate concentrations on a log scale across the entire concentration range, a clear shift in both apparent affinity and maximum sulfate reduction rates at concentrations between 100 and 500 μM is evident (Fig. 3c). We interpret these data as dual MM kinetics with high-affinity kinetics at low sulfate concentrations (<500 μM) determined from the progress curve experiment (Fig. 1) where K_m was 10.2 μM and V_{max} was 13.7 fmol cell^{-1} d^{-1}. For the low-affinity sulfate reduction expressed at sulfate concentrations above 500 μM, the best-fit K_m value was 147 μM and the V_{max} was 18.9 fmol cell^{-1} d^{-1} (these dual MM kinetics curves are shown in Fig. 3). In summary, the data show that *D. autotrophicum* reduce sulfate in the typical marine concentration range with a K_m that similar to what is reported for other marine strains. However at sulfate concentrations below 500 μM *D. autotrophicum* shifts its apparent K_m to a low concentration similar to K_m values reported for freshwater sulfate-reducing bacteria. The shift was immediate and not related to the prior growth conditions.

RT-PCR

We analyzed the expression level of eight putative membrane-bound sulfate transport proteins in *D. autotrophicum* to detect if the observed change in K_m was associated with a change in expression of any of these genes. The analyses were performed by standard RT-PCR assays with primer pairs (Table 1) targeting the respective genes on RNA extracted from *D. autotrophicum* cultures grown under low (μM) or high (mM) sulfate concentrations.

351 The expression level of the genes *rpoB*, *aprA* and *dsrB,* respectively encoding the RNA polymerase
352 and two key enzymes of the sulfate reduction pathway as well as 16S rRNA were used as references
353 for comparison of the expression level of the genes encoding putative sulfate transport proteins. The
354 results clearly showed a differential regulation of transcription of the genes coding for sulfate
355 transport proteins in cultures grown under high or low sulfate concentrations (Table 2,
356 Supplementary Figure S1). Two DASS family Na^+-dependent transporters (HRM2_38230 and
357 HRM2_38300) showed a high expression level only at low sulfate concentrations whereas another
358 DASS family transporter (HRM2_40290) was only expressed at high sulfate concentrations (Table
359 2, Supplementary Figure S1). The expression level of the H^+-dependent transporter HRM2_40360
360 was decreased when the sulfate concentration was limiting. A second member of the same
361 transporter family, HRM2_33490, was expressed at similar levels at both high and low sulfate
362 concentrations while a third member, HRM2_13280, was not expressed at all in our experiments.

363 The expression level of *dsrB* and *aprA* was high at both high and low sulfate concentrations
364 whereas *rpoB* showed a reduction in expression level under low sulfate concentrations; 16S rRNA
365 RT-PCR products was formed in equally high amounts at both sulfate concentrations (Table 2,
366 Supplementary Figure S1).

367

368 **DISCUSSION**

369 **High- and low-sulfate reduction kinetics in sulfate reducing bacteria**

370 Marine sulfate reducers have traditionally been ascribed a low affinity towards sulfate in
371 response to the high concentrations of sulfate in seawater. But our recent studies of sulfate reduction
372 kinetics in marine sediment have shown that the natural microbial community will change from
373 reduction of sulfate with low sulfate affinity at high concentrations, to high affinity kinetics when

374 sulfate is depleted (7). Whether the different affinities was due to different populations of SRB
375 expressing either high or low affinity sulfate reduction kinetics, or if the shift in affinity was a result
376 of regulation at the cellular level, was not resolved by the published experiments. The results
377 presented here with *D. autotrophicum* demonstrate that both high- and low-affinity kinetics can be
378 expressed in a single marine SRB species in response to the external sulfate concentration. The
379 high-affinity K_m value (2.6 μM sulfate) previously observed in sediment from Aarhus Bay is even
380 lower than the value now found for *D. autotrophicum* (8 μM sulfate) and also lower than those
381 found in many freshwater SRB strains with K_m values ranging from 3 to 32 μM (8-12, 34). This
382 indicates that *D. autotrophicum* is not the only marine SRB that can induce high affinity sulfate
383 reduction and that SRB that are even more efficient under sulfate-depleted conditions than *D.*
384 *autotrophicum* are present in marine sediment.

385 We found that *D. autotrophicum* change its K_m value when sulfate concentrations decreased
386 below 100-500 μM. This bears striking resemblance to previous studies of sulfate accumulation in
387 SRB cultures with blocked sulfate reduction. Stahlmann et al. (1991) (14) found that *D.*
388 *autotrophicum* had a maximum sulfate accumulation factor of ~1000 times ($C_{internal}/C_{ambient}$) with an
389 ambient sulfate concentration of 2.6 μM. The accumulation factor decreased to <30 when 1 mM
390 sulfate was added, which suggested a shift between two different sulfate uptake systems depending
391 on the ambient sulfate concentration. Similar observations were made for two freshwater SRB
392 species, *Desulfovibrio desulfuricans* and *Desulfobulbus propionicus,* and for the marine species,
393 *Desulfococcus multivorans*, and *Desulfovibrio salexigens,* as well (15, 16, 35, 36). In all cases the
394 accumulation factor increased substantially when the ambient concentration decreased below 100
395 μM. Common to these studies was that no kinetic experiments were performed (and no K_m values
396 could be reported) since sulfate reduction was blocked. The most likely link between sulfate
397 accumulation and reduction affinity is that accumulation will expose the enzymes in the cytoplasm

to increased sulfate concentrations. The effect is a decrease of the apparent K_m because this parameter is derived from the relation between the rates of reaction and the sulfate concentration in the environment. We believe that the capacity to shift from low- to high-affinity sulfate reduction kinetics, via a shift in uptake system, in response to decreasing ambient sulfate concentrations is not unique for *D. autotrophicum*. Other sulfate reducers in which the sulfate accumulation capacity is regulated in response to the ambient sulfate concentration (14) most likely also have dual apparent K_m.

Expression of membrane-bound sulfate transporters

Our identification of the shift in K_m in at low sulfate concentrations in *D. autotrophicum*, and the link between sulfate reduction kinetics and sulfate accumulation, led us to sceen the *D. autotrophicum* genome for membrane-bound sulfate transport proteins the differential expression of which could explain the response. The identity and kinetic properties of membrane-bound transporters involved in sulfate uptake in SRB are, however, poorly understood. By searching for homologs of transporters with a known function in assimilatory sulfate uptake across the cytoplasmic membrane in bacteria and eukaryotes we identified eight putative sulfate transporters encoded in the *D. autotrophicum* genome. All eight represent H^+-dependent (DASS family) or Na^+-dependent (SulP family) symporters, which agrees with the observation that *D. autotrophicum* cells power sulfate uptake electrochemically (14).

The expression pattern of the genes encoding the putative transporters was very reproducible for both high and low sulfate conditions (Table 2). Some of the transporters had clearly different expression levels under low and high sulfate conditions, which indicates that a high-affinity system was indeed induced when sulfate concentrations dropped below 70 µM, whereas at 15 mM a high-affinity system was closed down and a low-affinity system was active. Note that it would be

counterproductive for cells to have a highly accumulating transporter active at the same time as a less accumulating system because the electrochemically driven transporters are bidirectional. The sulfate pumped into the cytoplasm by the highly accumulating transporter would simply flow out through the low accumulating transporter at a net expence of one proton per sulfate molecule (or one equivalent sodium ion).

Members of the SulP family are generally characterized as H^+-dependent high-affinity sulfate symporters. For *D. autotrophicum* only one of these transporters, HRM2_40360 (SulP 3), was differentially expressed being down-regulated by sulfate limitation (Table 2), while another was expressed at both sulfate concentrations. Sulfate uptake in *D. autotrophicum* was shown to be Na^+-dependent, and not H^+- dependent (14), suggesting that the SulP symporters are not its primary sulfate transporters. Indeed two of the DASS family Na^+-dependent putative sulfate transporters showed increased expression levels at low sulfate concentrations (HRM2_38230 and HRM2_38300, Table 2). It should be noted that the DASS family transporters are typically attributed a function in uptake of divalent organic acids in bacteria (17). However, we hypothesize that HRM2_38230 and HRM2_38300 are involved in high-affinity sulfate transport since their expression increases at low external sulfate concentration. HRM2_38230 and HRM2_38300 are located in two small neighboring putative operons. Both operons include genes encoding two-component response regulators (HRM2_38210, HRM2_38290) and the HRM2_38230 operon also encodes a two-component sensory box histidine kinase/response regulator (HRM2_38220). This indicates that the expression of both transporters may respond to environmental changes. Similarly both the DASS family transporter HRM2_40290 and the SulP family transporter HRM2_40360, which were only expressed under high sulfate conditions (Table 2) also co-locate with genes encoding such sensory and regulatory proteins (HRM2_40310, HRM2_40320, HRM2_40330, HRM2_40340, HRM2_40350). In contrast such genes are not flanking the two other SulP family

transporters (HRM2_13280, HRM2_33490) or the DASS family transporter (HRM2_07790), which were not differentially expressed under high and low sulfate conditions (Table 2).

Metabolism of *D. autotrophicum* at sulfate concentrations below K_m

The low K_m values in *D. autotrophicum* show that a high-affinity sulfate-reducing system become active when sulfate becomes limiting. This challenges earlier studies that have proposed a threshold concentration for sulfate reduction by SRB although sulfate reduction would be thermodynamically feasible. Such threshold concentrations were found in the range of 2-36 μM for *D. postgatei* (13) and 5-10 μM for *D. salexigens* (10), hence both marine species were attributed a low affinity for sulfate. A sulfate threshold of 1.8 μM was found in two thermophilic freshwater SRB based on progress curve experiments showing high-affinity sulfate reduction kinetics with a low K_m value of 3 μM (12). When we estimated the residual sulfate pool based on the initial ratio of sulfate concentration to ^{35}S radioactivity we found what first appeared to be a threshold at 0.1-2 μM sulfate. With the additional distillation of the culture medium we could more efficiently separate the total reduced inorganic sulfur (^{35}S TRIS) from the ^{35}S sulfate and show that the threshold was largely due to ^{35}S TRIS that had escaped removal from solution by Zn precipitation and centrifugation. When correcting for this background, *D. autotrophicum* proved to deplete sulfate even down to a few nM. Thus, we found no treshold concentration above the thermodynamic limit and the relatively high threshold concentrations reported previously (10, 12, 13) might be due to experimental problems in the separation of sulfate and sulfide.

During the progress curve experiments the sulfate concentrations dropped from 70 μM to a few nM. Throughout this concentration range we observed that *dsrB* and *aprA* (Table 2), which are responsible for key steps in the dissimilatory sulfate reduction, remained expressed. The expression of *dsrB* and *aprA* when the concentration was only a few nM and net sulfate reduction had stopped

indicates that these genes are constitutively expressed in *D. autotrophicum,* which was also reported previously for *dsrB* in this species (37).

We found that the expression of the RNA polymerase (*rpoB*) was clearly reduced under sulfate limitation (Table 2) during progress curve experiments, which likely implies an overall reduction in cellular metabolic activity and gene expression in response to the low sulfate availability.

The limits of adaptation

According to the laws of thermodynamics the energy yield from chemical reactions decrease with decreasing concentration of reactants. Consequently, the sulfate reduction of *D. autotrophicum* cannot follow MM kinetics all the way to complete sulfate depletion and the reaction rate must taper off as the reaction approach thermodynamic equilibrium. The extent of thermodynamic control (*F*) can be calculated according to Jin and Bethke (38):

$$F = 1 - \exp\left(\frac{\Delta G_r}{RT}\right) \qquad \text{(Equation 5)}$$

Where ΔG_r is the Gibbs free energy of reaction, *R* is the gas constant and *T* is absolute temperature. *F* is an independent factor in a kinetic expression that takes into account the balance between forward and reverse reaction. Thus, *F* is 1 for a reaction far from thermodynamic equilibrium and approach zero as the reaction approaches thermodynamic equilibrium at $\Delta G_r = 0$. During the progress curve experiments with excess ethanol the calculated ΔG_r (equation 4) changed from -65 to -39 kJ mol^{-1} sulfate when the sulfate concentration dropped from 100 μM down to 1nM. According to Eq. 5 the forward drive of the reaction is approximately 1 and we expect no thermodynamic influence on the reaction rate. Sulfate reducers couple sulfate reduction to energy conservation via ATP generation. The minimum quantum of energy that can be coupled to ATP generation is ~10 kJ mol^{-1} reaction (38), leaving the energetic yield of the overall coupled reaction

493 at only -29 kJ mol^{-1}, but this is still sufficient to make the F approach 1. The reaction rate was
494 therefore not under thermodynamic control.
495 The applied concentration of electron donor (1 mM) in our experiments is, however, much
496 higher than can be expected for a sulfate depleted marine habitat. An important marine setting
497 where sulfate is depleted is the upper part of the methanogenic zone of coastal sediments. Here the
498 sulfate concentration may be in the range of 0 -100 μM and the concentration of the quantitatively
499 most important substrate, acetate, may be 10 μM (39). The pH is generally close to neutral, HS^-
500 may be up to 10 mM and HCO_3^- up to 40 mM (4, 7). Under those conditions, *F* is still high, 0.9, at a
501 sulfate concentration of 2 μM but decrease to 0.1 at 0.2 μM sulfate. Thermodynamic control may
502 thus start to play a role under *in situ* conditions when the sulfate concentration drops below 1 μM.
503 In conclusion, the high-affinity enzymatic systems responsible for uptake and reduction of sulfate in
504 *D. autotrophicum* are under kinetic control down to sulfate concentrations much below the K_m of 8
505 μM. The sulfate reduction operates down to sub-μM concentrations where the control on sulfate
506 reduction rate changes from kinetic to thermodynamic limitation in natural sulfate-depleted
507 environments. Such low sulfate concentrations may be reached only deep down beneath the main
508 sulfate zone of marine sediment, in the lower methane zone where also pore water sulfide has been
509 depleted (4).
510
511 **CONCLUSION**

512 *D. autotrophicum* changes its apparant K_m towards sulfate in response to the external sulfate
513 concentration. The mechanisem is via differential expression/regulation of sulfate transporters that
514 lead to relatively increased internal sulfate concentration in the cytoplasm at low concentrations in
515 the enviroment. The most likely regulated genes encoded for the DASS family of Na^+-dependent
516 transporters. The low accumulation system prevents high ambient sulfate concentrations from

causing excessive loading of the cytoplasm with sulfate and the concurrent increase in K_m has no effect on the rate of reaction at high sulfate concentrations. The high affinity system allows *D. autotrophicum* to operate efficiently at decreasing sulfate concentrations until thermodynamics dictate the reaction to stop. No other lower treshold concentration for sulfate reduction was observed. The dual K_m is most likely common among sulfate reducers and helps explain how sulfate reduction can proceed in marine sediments at very low sulfate concentrations such as in the sulfate-methane transition zone or the underlying methanogenic zone (4, 40).

Acknowledgements

We thank Kai Finster, Clemens Glombiza, and Kjeld Ingvorsen for constructive comments and helpful discussions during the project. We thank Jeanette Holm and Trine Bech Søgaard for excellent technical assistance. The study was funded by the Graduate School of Science and Technology of Aarhus University, the Danish National Research Foundation (grant agreement number DNRF104), the German Max Planck Society, and the European Research Council (ERC) Advanced Grant 'Microbial life under extreme energy limitation (MICROENERGY)' awarded to BBJ under the EU 7th FP.

REFERENCES

1 **Jørgensen BB.** 1982. Mineralization of organic-matter in the sea bed - the role of sulfate reduction. Nature **296**:643-645.

2 **Canfield DE, Kristensen E, Thamdrup B.** 2005. The sulfur cycle. Advances in Marine Biology **48**:313-381.

3 **Iversen N, Jørgensen BB.** 1985. Anaerobic methane oxidation rates at the sulfate methane transition in marine sediments from Kattegat and Skagerrak (Denmark). Limnology and Oceanography **30**:944-955.

4 **Holmkvist L, Ferdelman TG, Jørgensen BB.** 2011. A cryptic sulfur cycle driven by iron in the methane zone of marine sediment (Aarhus Bay, Denmark). Geochim Cosmochim Acta **75**:3581-3599.

5 **Cypionka H. 1994.** Sulfate transport. Inorganic microbial sulfur metabolism **243**:3-14.

6 **Button DK.** 1991. Biochemical basis for whole-cell uptake kinetics: specific affinity, oligotrophic capacity, and the meaning of the michaelis constant. Appl Environ Microbiol **57**:2033-2038.

7 **Tarpgaard IH, Røy H, Jorgensen BB.** 2011. Concurrent low- and high-affinity sulfate reduction kinetics in marine sediment. Geochim Cosmochim Acta **75**:2997-3010.

8 **Dalsgaard T, Bak F.** 1994. Nitrate reduction in a sulfate-reducing bacterium, *Desulfovibrio desulfuricans*, isolated from rice paddy soil - sulfide inhibition, kinetics, and regulation. Applied Environ Microbiol **60**:291-297.

9 **Fukui M, Takii S.** 1994. Kinetics of sulfate respiration by free-living and particle-associated sulfate- reducing bacteria. FEMS Microbiol Ecol **13**:241-247.

10 **Ingvorsen K, Jørgensen BB.** 1984. Kinetics of sulfate uptake by fresh-water and marine species of *Desulfovibrio*. Arch Microbiol **139**:61-66.

11 **Okabe S, Nielsen PH, Characklis WG.** 1992. Factors affecting microbial sulfate reduction by *Desulfovibrio desulfuricans* in continuous culture - limiting nutrients and sulfide concentration. Biotechnol Bioeng **40**:725-734.

12 **Sonne-Hansen J, Westermann P, Ahring BK.** 1999. Kinetics of sulfate and hydrogen uptake by the thermophilic sulfate-reducing bacteria *Thermodesulfobacterium* sp. strain JSP and *Thermodesulfovibrio* sp. strain R1Ha3. Appl Environ Microbiol **65**:1304-1307.

13 **Ingvorsen K, Zehnder AJB, Jørgensen BB.** 1984. Kinetics of sulfate and acetate uptake by *Desulfobacter postgatei*. Appl Environ Microbiol **47**:403-408.

14 **Stahlmann J, Warthmann R, Cypionka H.** 1991. Na^+-dependent accumulation of sulfate and thiosulfate in marine sulfate-reducing bacteria. Arch Microbiol **155**:554-558.

15 **Warthmann R, Cypionka H**. 1990. Sulfate transport in *Desulfobulbus porpionicus* and *Desulfococcus multivorans*. Arch Microbiol **154**:144-149.

16 **Kreke B, Cypionka H.** 1994. Role of sodium-ions for sulfate transport and energy-metabolism in *Desulfovibrio salexigens*. Arch Microbiol **161**:55-61.

17 **Saier MH, Jr., Tran CV, Barabote RD.** 2006. TCDB: The Transporter Classification Database for membrane transport protein analyses and information. Nucleic Acids Res **34**:D181-D186.

18 **Brysch K, Schneider C, Fuchs G, Widdel F.** 1987. Lithoautotrophic growth of sulfate-reducing bacteria, and description of *Desulfobacterium autotrophicum* gen. nov., sp. nov. Arch Microbiol **148**:264-274.

19 **Strittmatter AW, Liesegang H, Rabus R, Decker I, Amann J, Andres S, Henne A, Fricke WF, Martinez-Arias R, Bartels D, Goesmann A, Krause L, Puehler A, Klenk H-P, Richter M, Schueler M, Gloeckner FO, Meyerdierks A, Gottschalk G, Amann R.** 2009. Genome sequence of *Desulfobacterium autotrophicum* HRM2, a marine sulfate reducer oxidizing organic carbon completely to carbon dioxide. Environ Microbiol **11**:1038-1055.

20 **Mogensen GL, Kjeldsen KU, Ingvorsen K.** 2005. *Desulfovibrio aerotolerans* sp nov., an oxygen tolerant sulphate reducing bacterium isolated from activated sludge. Anaerobe **11**:339-349.

21 **Røy H, Weber HS, Tarpgaard IH, Ferdelman TG, Jørgensen BB.** 2014. Determination of dissimilatory sulfate reduction rates in marine sediment via radioactive 35S tracer. Limnol Oceanogr-Meth **12**:196–211.

22 **Jørgensen BB.** 1978. Comparison of methods for the quantification of bacteral sulfate reduction in coastal marine-sediments. 3. Estimation from chemical and bacteriological field data. Geomicrobiol J **1**:49-64.

23 **Markowitz VM, Chen IMA, Palaniappan K, Chu K, Szeto E, Grechkin Y, Ratner A, Jacob B, Huang J, Williams P, Huntemann M, Anderson I, Mavromatis K, Ivanova NN, Kyrpides NC.** 2012. IMG: the integrated microbial genomes database and comparative analysis system. Nucleic Acids Res **40**:D115-D122.

596 24 **Punta M, Coggill PC, Eberhardt RY, Mistry J, Tate J, Boursnell C, Pang N, Forslund**
597 **K, Ceric G, Clements J, Heger A, Holm L, Sonnhammer ELL, Eddy SR, Bateman A,**
598 **Finn RD.** 2012. The Pfam protein families database. Nucleic Acids Res **40**:D290-D301.

599 25 **Haft DH, Selengut JD, White O.** 2003. The TIGRFAMs database of protein families.
600 Nucleic Acids Res **31**:371-373.

601 26 **Tatusov RL, Natale DA, Garkavtsev IV, Tatusova TA, Shankavaram UT, Rao BS,**
602 **Kiryutin B, Galperin MY, Fedorova ND, Koonin EV.** 2001. The COG database: new
603 developments in phylogenetic classification of proteins from complete genomes. Nucleic
604 Acids Res **29**:22-28.

605 27 **Parra F, Britton P, Castle C, Jones-Mortimer MC, Kornberg HL.** 1983. Two separate
606 genes involved in sulphate transport in *Escherichia coli* K12. J Gen Microbiol **129**:357-358.

607 28 **Rückert C, Koch DJ, Rey DA, Albersmeier A, Mormann S, Puhler A, Kalinowski J.**
608 2005. Functional genomics and expression analysis of the *Corynebacterium glutamicum*
609 fpr2-cysIXHDNYZ gene cluster involved in assimilatory sulphate reduction. BMC
610 Genomics **6**:121.

611 29 **Altschul SF, Madden TL, Schaffer AA, Zhang JH, Zhang Z, Miller W, Lipman DJ.**
612 1997. Gapped BLAST and PSI-BLAST: a new generation of protein database search
613 programs. Nucleic Acids Res **25**:3389-3402.

614 30 **Gisin J, Mueller A, Pfaender Y, Leimkuehler S, Narberhaus F, Masepohl B.** 2010. A
615 *Rhodobacter capsulatus* member of a universal permease family imports molybdate and
616 other oxyanions. J Bacteriol **192**:5943-5952.

31 **Mansilla MC, de Mendoza D.** 2000. The *Bacillus subtilis* cysP gene encodes a novel sulphate permease related to the inorganic phosphate transporter (Pit) family. Microbiology **146**:815-821.

32 **Kibbe WA.** (2007) OligoCalc: an online oligonucleotide properties calculator. Nucleic Acids Res **35**:W43-W46

33 **Muyzer G, Dewaal EC, Uitterlinden AG.** 1993. Profiling of complex microbial populations by denatuing gradient gel-electrophoresis analysis of polymerase chain reaction-amplified genes coding for 16S ribosomal RNA. Appl Environ Microbiol **59**:695-700.

34 **Nethejaenchen R, Thauer RK.** 1984. Growth yields and saturation constants of *Desulfovibrio vulgaris* in chemostat culture. Arch Microbiol **137**:236-240.

35 **Kreke B, Cypionka H.** 1992. Protonmotive force in freshwater sulfate-reducing bacteria, and its role in sulfate accumulation in *Desulfobulbus propionicus*. Arch Microbiol **158**:183-187.

36 **Cypionka H.** 1989. Characterization of sulfate transport in *Desulfovibrio desulfuricans*. Arch Microbiol **152**:237-243.

37 **Neretin LN, Schippers A, Pernthaler A, Hamann K, Amann R, Jørgensen BB.** 2003. Quantification of dissimilatory (bi)sulphite reductase gene expression in *Desulfobacterium autotrophicum* using real-time RT-PCR. Environ Microbiol **5**:660-671.

38 **Jin QS, Bethke CM.** 2003. A new rate law describing microbial respiration. Appl Environ Microbiol **69**:2340-2348.

637 39 **Jørgensen BB, Parkes RJ.** 2010. Role of sulfate reduction and methane for anaerobic
638 carbon cycling in eutrophic fjord sediments (Limfjorden, Denmark). Limnol Oceanogr
639 **55**:1338-1352.

640 40 **Leloup J, Loy A, Knab NJ, Borowski C, Wagner M, Jørgensen BB.** 2007. Diversity and
641 abundance of sulfate-reducing microorganisms in the sulfate and methane zones of a marine
642 sediment, Black Sea. Environ Microbiol **9**:131-142.
643

644 **FIGURES**

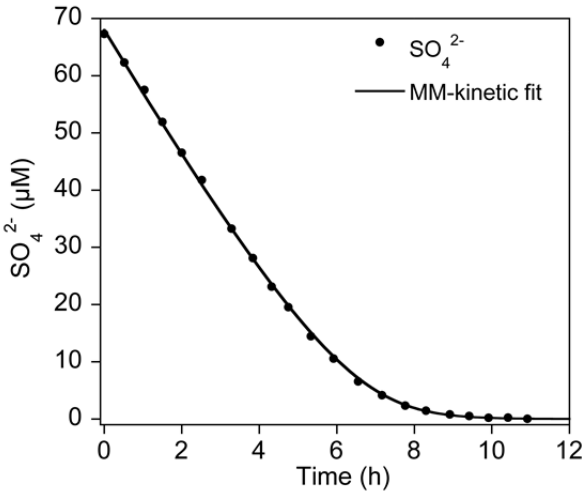

645 **Fig. 1**. Example of progress curve experiment with *D. autotrophicum* made after a fed batch pre-
646 incubation II (see text). Sulfate radioactivity was measured at regular time intervals and sulfate
647 concentrations were calculated based on the initial sulfate:radioactivity ratio. The data closely
648 follow Michaelis-Menten kinetics. The maximum rate (V_{max}) and the apparent half saturation
649 constant (K_m) determined by a least squares fit (curve shown) using Eq. 2 were 12.8 μM h^{-1} and
650 10.2 μM, respectively. Based on microscopic cell counts, the calculated cell-specific V_{max} was 14.2
651 fmol $cell^{-1}$ d^{-1}.

652

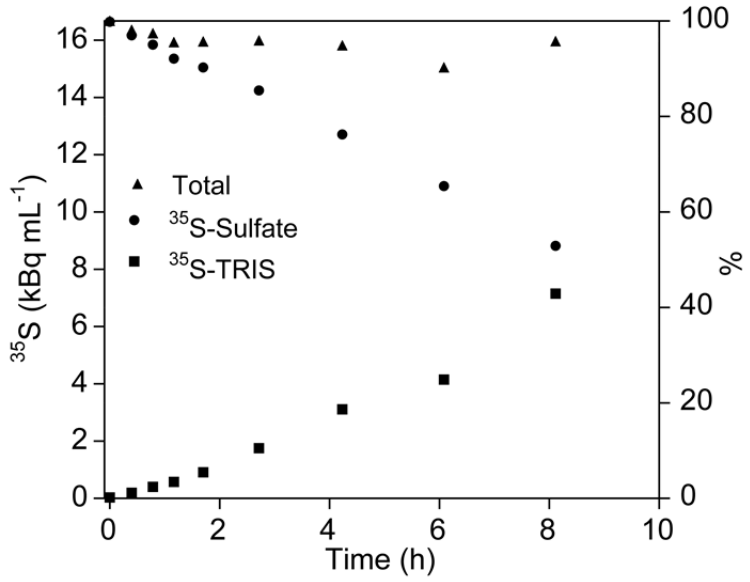

Fig. 2. First part of a progress curve experiment with *D. autotrophicum*. The ^{35}S radioactivities were measured in both the free sulfate pool (^{35}S sulfate) and the total reduced sulfur pool (^{35}S TRIS). The sum of the two pools (Total) was in average 96% of the initial value over the course of the experiment. The two concentration scales show to the left the radioactivities in kBq mL^{-1} and to the right the % of initial total radioactivity.

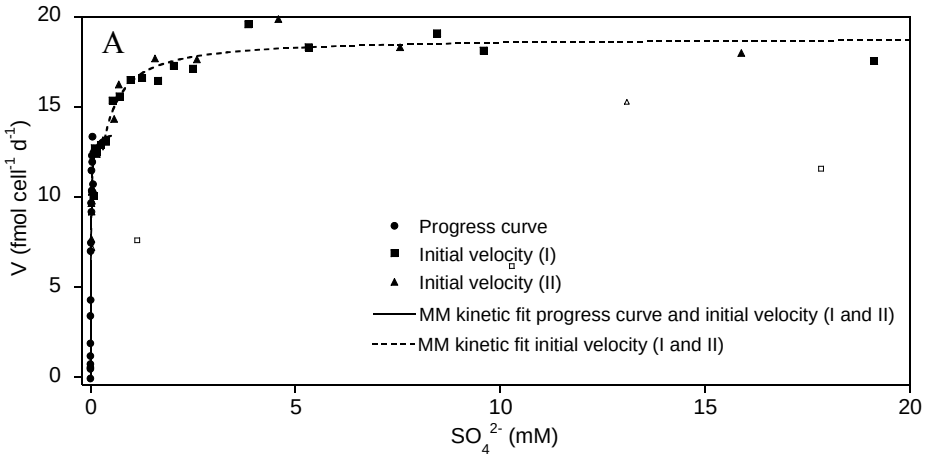
A
V (fmol cell^{-1} d^{-1})
SO_4^{2-} (mM)
Progress curve
Initial velocity (I)
Initial velocity (II)
MM kinetic fit progress curve and initial velocity (I and II)
MM kinetic fit initial velocity (I and II)

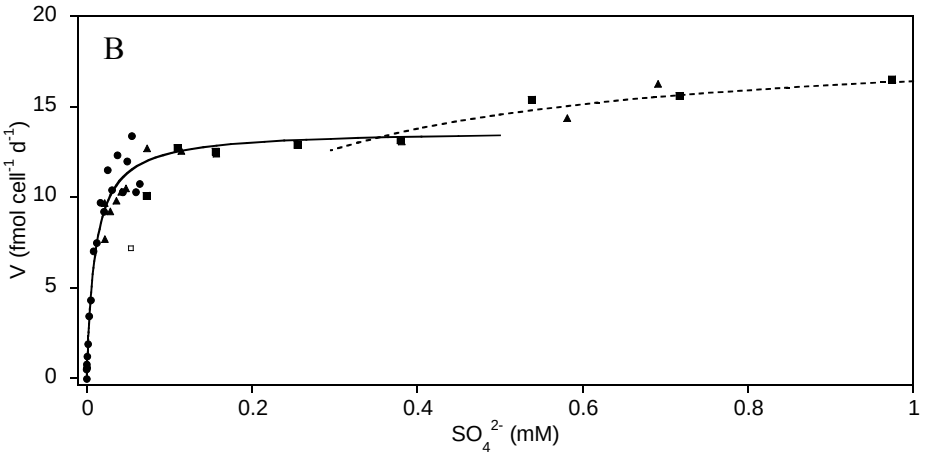
B
V (fmol cell^{-1} d^{-1})
SO_4^{2-} (mM)

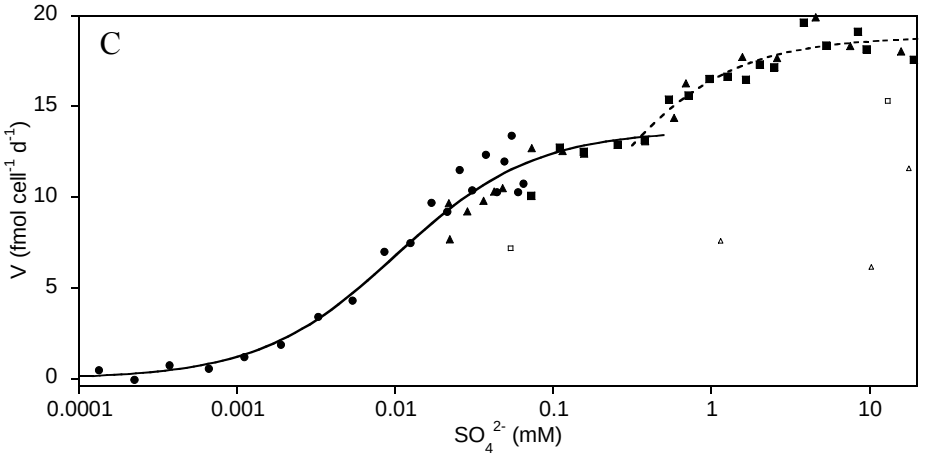
C
V (fmol cell^{-1} d^{-1})
SO_4^{2-} (mM)

664

665 **Fig 3**. Combined high- and a low-affinity Michaelis-Menten kinetics fit to data from two initial-
666 velocity experiments (I and II) and one progress curve experiment (from Fig 1.). The same data are
667 plotted as cell specific rates in fmol SO_4^{2-} $cell^{-1}$ day^{-1} on three different concentration scales: a) 0 -
668 20 mM linear, ;b). 0-1 mM linear, and c) 0.1 μM to >10 mM on a log scale. Both high- and low-
669 affinity Michaelis-Menten curves are shown in all plots. Outlying data considered to be
670 experimental error are marked with open symbols and are not included in the non-linear least
671 squares fit.

672 TABLES

673 Table 1. Gene targets and primers used for RT-PCR. for, forward; rev, reverse (5´ - 3´).

Locus Tag*	**Transporter family**	**Gene product name***	**Primers**	**Basic $T_{melting}$ (C°)#**	**PCR amplicon size (bp)**
HRM2_40290	DASS TIGR00785	Na^+-dependent di and tricarboxylate transporter/sulfate sodium-cotransporter	for: TTTCTCATGGCCGGAACC rev: TAGGCCATGCCGATGAAC	50.3 50.3	410
HRM2_07790	DASS TIGR00785	Na^+-dicarboxylate cotransporter (solute carrier 13)	for: ACGGTTGGCGCTTTTGAC rev: TGCCGGCCGATAGATGAG	50.3 50.3	418
HRM2_38230	DASS TIGR00785	High-affinity sodium/sulfate dependent symporter NadC1	for: TTCTTGCCCCTGGTTACC rev: CCCCCAAACTTTGGAAGC	50.3 50.3	416
HRM2_38270	DASS TIGR00785	High-affinity sodium/sulfate dependent symporter NadC2	for: TACCCAACGTGCGATGG rev: TTCCCGCTTCAGGTGATC	50.3 50.3	416
HRM2_38300	DASS TIGR00785	High-affinity sodium/sulfate dependent symporter NadC3	for: CATGACGCCACCATAACC rev: TGAACCAGAGCAGGAAGG	50.3 50.3	412
HRM2_13280	SulP TIGR00815	High-affinity H^+/sulfate cotransporter SulP1	for: CAGCTTGTCCAGGGAATGGT rev: AGGTTGGCAAGACCCATGGA	53.8 53.8	419
HRM2_33490	SulP TIGR00815	High-affinity H^+/sulfate cotransporter SulP2	for: TGGCCTTGCAAAGCTTGG rev: GGGCAAGCATTCGTAGTG	50.3 50.3	413
HRM2_40360	SulP TIGR00815	High-affinity H^+/sulfate cotransporter SulP3	for: GTTGCTGTGACCATCGTGA rev: AAGCAGTCGGTTACTCACCT	51.4 51.8	419
HRM2_36320 *rpoB*	-	DNA-directed RNA polymerase, beta chain RpoB	for: CCAATTGAGACTCCTGAGG rev: CGCTGCATGTTAGAACCCAT	51.1 51.8	382
HRM2_42390 *dsrB*	-	Dissimilatory sulfite reductase complex, beta subunit, DsrB	for: CAACATTGTTCATACCCAGG rev: GGTGTAGCAGTTACCGCAG	49.7 53.2	380
HRM2_04510 *aprA*	-	Adenosine-5`-phosphosulfate reductase, alpha subunit, AprA	for: ATGGCAGATCATGATCAATGG rev: GGACATGTCAAGGAAATCTTC	50.5 50.5	689
16S rRNA§	-	16S ribosomal RNA	for: CCTACGGGAGGCAGCAG** rev: CCGTCAATTCCTTTRAGTTT**	54.3 46-48	587

674 **Desulfobacterium autotrophicum* HRM2 genome sequence (CP001087).

675 [#]Calculated by OligoCalc: (32). All primer pairs were applied at an annealing temperature of 57 ^{o}C.

676 [§]Locus tags: HRM2_22530, HRM2_29680, HRM2_34900, HRM2_35110, HRM2_46980, HRM2_47050.

677 **Reference (33).

678

679 Table 2. Transcription level of potential membrane-bound sulfate transport proteins in *D. autotrophicum* grown under high sulfate
680 concentrations in five different batch experiments and under low sulfate concentrations in four different progress curve experiments.
681 Representative agarose gel pictures of RT-PCR products are shown in supplementary Fig. S1. Lac, lactate; Eth, ethanol; n, number of RT-
682 PCR on that template; ND, not determined; *rpoB*, RNA polymerase; *dsrB*, Dissimilatory sulfite reductase; *aprA*, Adenosine-5`-
683 phosphosulfate reductase. Gene product names of the shown genome locus tags are presented in Table 1.
684

Growth-conditions[§1]	**n**	**DASS family, Na^+-dependent transporters**					**SulP family, H^+-dependent transporters**			**Reference genes**[§2]		
		HRM2_40290	HRM2_07790	HRM2_38230	HRM2_38270	HRM2_38300	HRM2_13280	HRM2_33490	HRM2_40360	*rpoB*	*dsrB*	*aprA*
LOW sulfate												
Progress curve Lac (<100nM sulfate)	3	-	+	+++	++++	+++	-	+	-	++	+++	++++
Progress curve Lac (<100nM sulfate)	3	-	++	++	++++	++	-	+	-	+	++++	ND
Progress curve Eth (70 µM sulfate)	2	-	+	++	+++	++	-	-	-	+	+++	+++
Progress curve Eth (70 µM sulfate)	3	-	+	++	+++	++	-	+	-	+	+++	++++
HIGH sulfate (~15 mM)												
Batch culture Lac	1	++	+	-	+++	-	ND	+	ND	++++	++++	++++
Batch culture Eth	3	+++	+	-	++	-	-	+	++	++++	++++	++++
Batch culture Eth	2	++	++	+	++	+	-	+	++	++++	++++	++++
Batch culture Eth	2	+++	++	+	+++	-	ND	+	ND	++++	++++	ND
Batch culture Eth	3	+++	+	+	+++	+	-	+	++	++++	++++	++++

685 [§1] All cells from progress curve experiments experienced only ethanol during the final 12 hours before sampling for RNA.

686 [§2]16S rRNA was present in high abundance in RT-PCR products from both high and low sulfate cultures.